Control No. AP147

MATHEMATICAL MODEL OF CONTAMINANT TRANSPORT THROUGH FRACTURE-POROUS MATRIX SYSTEM

by

A.G. Bobba

Aquatic Physics and Systems Division

National Water Research Institute

Burlington, Ontario, Canada

L7R 4A6

NWRI Contribution #86-21

MATHEMATICAL MODEL OF CONTAMINANT TRANSPORT THROUGH FRACTURE-POROUS MATRIX SYSTEM

by

A.G. Bobba

Aquatic Physics and Systems Division

National Water Research Institute

Burlington, Ontario, Canada

L7R 4A6

ABSTRACT

A mathematical model for determining solute concentrations at a point within a cylindrically symmetrical conduit fracture/porous matrix system is described. Both convective and dispersive propagation is considered within the fracture subsystem, while only dispersive propagation is considered with the porous matrix subsystem. The two subsystems are coupled through continuity restrictions imposed at their interface boundary. The transport equations are then subjected to dimensionless analyses and solved utilizing an alternating direction implicit method technique. The dimensionless solute concentration profiles resulting from this model are then sketched and discussed.

EXECUTIVE SUMMARY

Recently, the problem of contaminant transport in fractured porous formations has attracted considerable attention in many countries, especially when dealing with the disposal of radioactive waste in underground repositories. A mathematical model for determining solute concentrations at a point within a cylindrically symmetrical conduit fracture/porous matrix system is described. Both convective and dispersive propagation is considered within the fracture subsystem, while only dispersive propagation is considered with the porous matrix subsystem. The two subsystems are coupled through continuity restrictions imposed at their interface boundary. The transport equations are then subjected to dimensionless analyses and solved utilizing an alternating direction implicit method technique. The dimensionless solute concentration profiles resulting from this model are then sketched and discussed.

INTRODUCTION

Disposing of high level radioactive wastes in deep underground depends upon the ability of the natural rock to isolate radioactivity from the biosphere. Attractive geologic conditions are natural salt deposits, which are free of groundwater, of granites, shales, and other media which are subject to little or no movement of natural groundwater. The concentrated wastes will be cast into solids, such as glass, and encased in metal containers. This waste container is expected to last for hundreds and thousands of years underground without appreciable deterioration.

The migration of radioactive waste in various kinds of rocks has become an area of large interest in the last decade because of various national and international efforts in studying the final disposal of radioactive wastes from nuclear power plants. The crystalline rocks are selected in Canada, and other European countries as the most suitable bedrock in which to build a repository. In crystalline rock the water moves through fractures which may be fairly far apart at deeper formations. The radionuclides transported by groundwater will interact in various ways with the rock. They may be strongly retarded due to adsorption on the surface of the fracture and after a long time, it may also penetrate the intercrystalline of the porous matrix of the rock.

Despite the realization of the importance of fractured media in the overall detailed descriptions of the dispersive and convective propagation of contaminants through subsurface water systems (e.g., Day, 1977; Snow, 1969; Grisak et al., 1980a; Wilson and Witherspoon, 1970, Neretneiks, 1980; Rasmuson and Nereknieks, 1981; Tang et al., 1981; Sudicky and Frind, 1982; Rasmuson, 1984; and Neretrnieks and Rasumson, 1984), until recently, surprisingly little modelling effort has been directed towards the effects the presence of such physical fractures produce upon the contaminant flow through porous subsurface media. Grisak and Pickens, 1980b and Grisak et al., 1980, have recently reported the results of both theoretical and experimental studies directed towards an evaluation of the processes pertinent to the transport of solutes through fractured media. Their work has provided an excellent opportunity for illustrating the effects of hydrogeologic parameters on the concentration profiles of groundwater systems containing fractures into which solutes have been intruded.

The object of this paper is to present the results of contaminant transport through a fracture/porous matrix.

THE MASS TRANSPORT MODEL

Figure 1 schematically illustrates the fracture/porous matrix system considered in this analysis. The fracture is considered as a cylindrical conduit of variable radius r_o. A cylindrical

coordinate system is established with an origin O at the centre of the conduit. The z-axis is defined as the axis of rotation of the cylinder, and the r-axis is perpendicular to the z-axis at each point along the z-axis. Groundwater is considered to enter the fracture with a constant velocity V (in the range $-r_o < r > r_o$) along the positive z direction. The homogeneous porous medium completely surrounds the conduit in a symmetrical manner and extends to a distance r_{max} where $r_{max} > r_o$. The solute in the conduit fracture (phase I) is considered to be transported through the combined processes of convection and diffusion, while the solute in the porous matrix (phase II) is considered to be transported by radial and axial diffusion only. That is, the convective velocity in the axial direction everywhere in phase II is taken to be zero at all times. The initial (time t = 0) solute concentration in both phase I and phase II is taken to be zero, and solute is considered to enter the porous matrix in the radial direction by means of molecular diffusion across the phase I/phase II interface boundary

Mathematical simulation of such a mass transport system is, of course, further complicated by the fact that a complete system is involved. The nature of the propagative transport in each phase of the system both impacts and is impacted by the nature of the propagtive transport in the other phase. An attempt is made to incorporate such coupled system influences within the present model.

A brief summation of the assumptions of this model thus becomes:

a) A fully developed laminar flow is considered to enter the conduit fracture in the positive axial direction.

b) Negligible flow (convective velocity = 0) is considered to exist within the porous matrix.

c) The fracture/porous matrix system is considered to possess cylindrical symmetry.

d) The physical and chemical properties of all materials are considered to be constant in both space and time.

e) Both convection and diffusion processes determine solute transport within the fracture, while molecular diffusion is considered to determine radial transport across the interface boundary into either phase I or phase II.

f) All diffusion is taken to be described by Fick's First Law.

Following Jost, (1960), the cylindrical coordinate expression of the diffusion/convection mass transport equation governing solute propagation within the conduit fracture sub-system (phase I) may be written as

$$\frac{\partial C}{\partial t} = D_r^I \left[\frac{\partial^2 C}{\partial r^2} + \frac{1}{r}\frac{\partial C}{\partial r}\right] + D_Z^I \frac{\partial^2 C}{\partial z^2} - V_Z^I \frac{\partial C}{\partial z} \qquad (1)$$

and the mass transport equation governing solute propagatoin within the porous matrix sub-system (phase II) may be written as

$$\frac{\partial C}{\partial t} = D_r^{II}\left[\frac{\partial^2 C}{\partial r^2} + \frac{1}{r}\frac{\partial C}{\partial r}\right] + D_Z^{II}\frac{\partial^2 C}{\partial z^2} \qquad (2)$$

where C = solute concentration (ML^{-3})

D_r^I = radial diffusion coefficient in phase I (L^2T^{-1})

D_r^{II} = radial diffusion coefficient in phase II (L^2T^{-1})

D_Z^I = axial diffusion coefficient in phase I (L^2T^{-1})

D_Z^{II} = axial diffusion coefficient in phase II (L^2T^{-1})

V_Z = local velocity in phase I (LT^{-1})

r and z = cylindrical coordinate variables (L)

t = time (T)

M, L, and T refer to units of mass, length and time, respectively.

Physical coupling between the two phases is taken to be defined by the interace boundary conditions

$$C^I = C^{II} \text{ at } r = r_o \qquad (3)$$

and

$$D_r^I\left[\frac{\partial C}{\partial r}\right]^I = D_r^{II}\left[\frac{\partial C}{\partial r}\right]^{II} \text{ at } r = r_o \qquad (4)$$

The initial conditions of solute concentration may be taken as $C = 0$ for $t < 0$, $0 \leq r \leq r_{max}$, and $0 \leq Z \leq L$,

and $C = C_o$ for $t \geq 0$, $0 \leq r \leq r_o$ and $Z = 0$

where L is the axial length of the conduit fracture. It will be shown that the selection of such initial conditions in no way inhibits the rapid development of a parabolic velocity profile within the fracture.

The boundary conditions for the development of the current model are taken as:

$$C = C_o \qquad t \geq 0 \qquad 0 \leq r \leq r_o \qquad z = 0$$

$$\frac{\partial C}{\partial r} = 0 \qquad t \geq 0 \qquad r = 0 \qquad 0 \leq Z \leq L \tag{5}$$

$$\frac{\partial C}{\partial r} = 0 \qquad t \geq 0 \qquad r = r_{max} \qquad 0 \leq Z \leq L$$

$$\frac{\partial C}{\partial Z} = 0 \qquad t \geq 0 \qquad r_o \leq r \leq r_{max} \qquad Z = 0$$

$$\frac{\partial C}{\partial Z} = 0 \qquad t \geq 0 \qquad r_o \leq r \leq r_{max} \qquad Z = L$$

Since laminar flow is assumed within the fracture, the local velocity, V_Z may be expressed as

$$V_Z = V_m \left[1 - \left(\frac{r}{r_o}\right)^2\right] \tag{6}$$

where V_m is the maximum velocity observed along the z-axis.

The governing equations of the mass transport phenomena are now subjected to a dimensionless analysis by introducing the following dimensionless variables

$$r^* = \frac{r}{L_C};\ Z^* = \frac{Z}{L_C};\ V^* = \frac{V_Z}{V_C} \tag{7}$$

$$t^* = \frac{tV_C}{L_C};\ X = \frac{C}{C_o}$$

$$= \frac{t}{t_i},\ \text{where } t_i = \frac{L_C}{V_C}$$

where L_C and V_C represent a characteristic length and velocity, respectively, of the coupled subsystems.

Substituting (7) into (1) yields the dimensionless mass transport equation for the conduit fracture (phase I)

$$\frac{\partial C^*}{\partial t^*} = \frac{1}{p_r^I}\left[\frac{\partial^2 C^*}{\partial r^{*2}} + \frac{1}{r^*}\frac{\partial C^*}{\partial r^*}\right] + \frac{1}{p_z^I}\frac{\partial^2 C^*}{\partial Z^{*2}} - V^*\frac{\partial C^*}{\partial Z^*} \tag{8}$$

where $P_r^I = \frac{L_C V_C}{D_r^I}$ and $P_z^I = \frac{L_C V_C}{D_z^I}$ are

readily recognized as the dimensionless Peclet numbers appropriate to radial and axial solute transport within Phase I.

Similarly, substituting (7) into (2) yields the dimensionless mass transport equation for the porous matrix (phase II)

$$\frac{\partial C^*}{\partial t^*} = \frac{1}{P_r^{II}} \left[\frac{\partial^2 C^*}{\partial r^{*2}} + \frac{1}{r^*} \frac{\partial C^*}{\partial r^*}\right] + \frac{1}{P_z^{II}} \frac{\partial^2 C^*}{\partial z^{*2}} \qquad (9)$$

where $P_r^{II} = \frac{L_C V_C}{D_r^{II}}$ and $P_z^{II} = \frac{L_C V_C}{D_Z^{II}}$ are in

a form similar to the Peclet numbers P_r^I and P_Z^I.

Further, equations (3) and (4) defining the interface boundary conditions assume the dimensionless forms

$$C^{*I} = C^{*II} \text{ at } r^* = \frac{r_o}{L_C} \qquad (10)$$

and

$$\frac{1}{P_r^I}\left[\frac{\partial C^*}{\partial r^*}\right] = \frac{1}{P_r^{II}}\left[\frac{\partial C^*}{\partial r^*}\right] \text{ at } r^* = \frac{r_o}{L_C} \tag{11}$$

respectively.

Expressing the local velocity V_Z from equation (6) in dimensionless form yields

$$V^* = \frac{V_m}{V_C}\left[1 - \left(\frac{L_c r^*}{r_o}\right)^2\right] \tag{12}$$

Equations (9) to (12) then become the working equations for the current fracture/porous matrix model. Clearly it is seen that any solution to these equations will be functionally dependent upon the pair of Peclet numbers P_r^I and P_r^{II} appropriate to radial solute transport and the pair of Peclet numbers P_Z^I and P_Z^{II} appropriate to axial solute transport within the complex system.

The initial conditions and boundary conditions, expressed in dimensionless form become

$$C^* = 0 \quad t^* \leq 0 \quad 0 \leq r^* \quad \frac{r_{max}}{L_C} \qquad 0 \leq Z^* \leq \frac{L}{L_C}$$

$$C^* = 1 \quad t^* \geq 0 \quad 0 \leq r^* \leq \frac{r_o}{L_C} \qquad Z^* = 0$$

$$\frac{\partial C^*}{\partial r^*} = 0 \quad t^* \geq 0 \qquad r^* = 0 \qquad 0 \leq Z^* \leq \frac{L}{L_C} \qquad (13)$$

$$\frac{\partial C^*}{\partial r^*} = 0 \quad t^* \geq 0 \qquad r^* = \frac{r_{max}}{L_C} \qquad 0 \leq Z^* \leq \frac{L}{L_C}$$

$$\frac{\partial C^*}{\partial Z^*} = 0 \quad t^* \geq 0 \qquad \frac{r_o}{L_C} \leq r^* \leq \frac{r_{max}}{L_C} \qquad Z^* = 0$$

$$\frac{\partial C^*}{\partial Z^*} = 0 \quad t^* \quad 0 \qquad \frac{r_o}{L_C} \quad r^* \quad \frac{r_{max}}{L_C} \qquad Z^* = \frac{L}{L_C}$$

Similarity requirements are readily seen to be satisfied by replacing L_C by 2 r_o in the boundary conditions of equation (13) which now becomes

$$C^* = 0 \quad t^* \quad 0 \qquad 0 \quad r^* \quad \frac{r_{max}}{2r_o} \qquad 0 \quad Z^* \quad \frac{L}{2r_o}$$

$$C^* = 1 \quad t^* \quad 0 \qquad 0 \quad r^* \quad \frac{1}{2} \qquad Z^* = 0$$

$$\frac{\partial C^*}{\partial r^*} = 0 \quad t^* \quad 0 \qquad r^* = 0 \qquad 0 \quad Z^* \quad \frac{L}{2r_o} \tag{14}$$

$$\frac{\partial C^*}{\partial r^*} = 0 \quad t^* \quad 0 \qquad r^* = \frac{r_{max}}{2r_o} \qquad 0 \quad Z^* \quad \frac{L}{2r_o}$$

$$\frac{\partial C^*}{\partial Z^*} = 0 \quad t^* \quad 0 \qquad \frac{1}{2} \quad r^* \quad \frac{r_{max}}{2r_o} \qquad Z^* = 0$$

$$\frac{\partial C^*}{\partial Z^*} = 0 \quad t^* \quad 0 \qquad \frac{1}{2} \quad r^* \quad \frac{r_{max}}{2r_o} \qquad Z^* = \frac{L}{2r_o}$$

It is also readily seen that the selection of $V_C = V_m$ eliminates the functional dependence of concentration on velocity. Equation (12) may now be rewritten as the parabolic equation

$$V^* = 1 - 4r^{*2} \tag{15}$$

With the above choices of characteristic length and characteristic velocity, the mass transport equations for which numerical solutions are sought become

$$\frac{\partial C^*}{\partial t^*} = \frac{1}{P_r^I}\left[\frac{\partial^2 C^*}{\partial r^{*2}} + \frac{1}{r^*}\frac{\partial C^*}{\partial r^*}\right] + \frac{1}{P_Z^I}\frac{\partial^2 C^*}{\partial Z^{*2}} - (1-4r^{*2})\frac{\partial C^*}{\partial Z^*} \quad (16)$$

$$\frac{\partial C^*}{\partial t^*} = \frac{1}{P_r^{II}}\left[\frac{\partial^2 C^*}{\partial r^{*2}} + \frac{1}{r^*}\frac{\partial C^*}{\partial r^*}\right] + \frac{1}{P_Z^{II}}\frac{\partial^2 C^*}{\partial Z^{*2}} \quad (17)$$

$$C^{*I} = C^{*II} \text{ at } r^* = \frac{1}{2} \quad (18)$$

$$\frac{1}{P_r^I}\left[\frac{\partial C^*}{\partial r^*}\right] = \frac{1}{P_r^{II}}\left[\frac{\partial C^*}{\partial r^*}\right] \text{ at } r^* = \frac{1}{2} \quad (19)$$

Clearly, problems will arise in the numerical solution of equation (16) when $r^* = 0$, i.e., when axial positives in phase I are considered (this problem will not arise in equation (17), of course, since $r^* \neq 0$ at any point in phase II).

Applying L'Hospital's rule to the $\frac{1}{r^*}\frac{\partial C^*}{\partial r^*}$ term in equation (17) yields

$$\lim_{r^* 0} \frac{1}{r^*}\frac{\partial C^*}{\partial r^*} = \frac{\frac{\partial}{\partial r^*}\frac{\partial C^*}{\partial r^*}}{\frac{\partial}{\partial r^*} r^*} = \frac{\partial^2 C^*}{\partial r^{*2}} \quad (20)$$

Thus, for $r^* = 0$, the form of equation (16) utilized in obtaning numerical solutions for the mass transport equation is

$$\frac{\partial C^*}{\partial t^*} = \frac{2}{P_r^I}\frac{\partial^2 C^*}{\partial r^{*2}} + \frac{1}{P_Z^I}\frac{\partial^2 C^*}{\partial Z^{*2}} - (1-4r^{*2})\frac{\partial C^*}{\partial Z^*} \qquad (16a)$$

NUMERICAL SOLUTION

Many of the differential equations resulting from a consideration of physical problems in applied science and engineering have no known analytical solutions, and must therefore be solved by employing numeical approximation techniques. Equations (16) to (20) include parabolic equations and a discussion of the various techniques available for obtaining approximate solutions to such second order partial differential equations is given by Jon Rosenberg (1968). Several of these available techniques involve an iteration procedure. However, such iterative techniques are impractical for the unsteady-state situations encountered in the current model, due largely to the excessive computation times required to obtain a solution. Consequently, the far less time-consuming alternating directon implicit method (ADIM) developed by Peaceman and Rachford (1955) was adopted in this work.

The ADIM approach to the solution of equations (16) to (20) involves the alternate implicit differencing of one parameter (Z* direction in the current work) and explicit differencing of the others (r* direction at t* time domain). It requires a sequential solution of a small set of simultaneous equations that may be approached through direct non-iterative procedures. Ananthakrisnan et al (1965)

have modified the ADIM for applicability to laminar dispersion in capillaries. By combining the original work of Peaceman and Rachford (1955) with the modified version of ADIM of Ananthakrishnan et al (1965), the alternating direction implicit method may be rendered suitable for use with the current coupled fracture/porous matrix system. Detailed discussion of the ADIM mathematical procedures developed for obtaining solutions to the transport equations and boundary conditions of the current model will be presented elsewhere, suffice to say that a grid network was established to cover the range of variables defining the coupled system, and the solute concentration was determined at each location within this grid network.

Alternate implicit differencing in the Z* direction and explicit differencing in the r* direction was performed. The concentration at each grid point was assumed to be initially zero. Subsequent to the introduction of a step change in solute concentration into the predominantly convection stream of the conduit fracture subsystem, t* was increased by a pre-determined increment and new values of solute concentration were computed from the Z* implicit equations. Utilizing the r* explicit equations and the same value of pre-determined t* increment, the solute concentrations were once again determined. This process was repeated until the desired time value was reached.

CONCENTRATION PROFILES

Using the preceding numerical methods, solutions for solute concentrations were obtained for a conduit fracture/porous matrix coupled system defined by $P_r^I = P_Z^I = 200$; $P_r^{II} = 100$; and $P_Z^{II} = 50$. These Peclet numbers are consistent with realistic anticipated values of V_m (.....?) for such fracture systems.

Figures 2 and 3 illustrate the transient axial solute concentration profiles for the fracture subsystem (Phase I) for $r^* = 0.25$ (i.e., $r = \frac{r_o}{2}$) and $r^* = 0$ (i.e., $r = 0$), respectively. The well-defined front produced by the step-change input is clearly evident within the fracture for small values of time T, the consequence of the predominance of the convective transport mechanism over the diffusive transport mechanism in phase I. The discontinuity associated with this front remains relatively intact to large values of T as the solute is transported through the conduit fracture. The frontal discontinuity at $r^* = 0.25$ (i.e., at a point midway between the radial axis and the interface between phases I and II) clearly lags the frontal discontinuity at $r^* = 0$ (i.e., at a point on the radial axis). This results in a parabolic velocity profile being observed within the conduit fracture subsystems, as illustrated in Figure 4 (obtained from equation (15)). Thus, even though a constant

(in r and z) laminar flow rapidly assumes the faimilar parabolic velocity profile once the solute has entered phase I. The effect of diffusion, directed radially outward from the axis of the conduit and acting to disperse the frontal discontinuity, is also clearly evident in Figures 2 and 3. As the discontinuity passes completely out of the fracture and into the porous matrix (phase II), the axial profiles assume a near-horizontal configuration.

Figure 5 illustrates the transient axial solute concentration profiles along the interface boundary between phase I and II for $r^* = r_o = 0.5$ at various dimensionless times T^*. Similar evolution of concentration profiles with time are evident at the interface as are evident within phase I except that the frontal discontinuity undergoes more rapid dissipation from the interface due to the reinforcing influence of the diffusion into the porous matrix. The conductive velocity log of the frontal discontinuity at the interface boundary is quite pronounced, a direct consequence of the parabolic velocity profile within the conduit fracture.

The response of the conduit fracture system is fully established prior to the intrusion of significant solute into the porous matrix subsystem (phase II) in the current example since the selection of Peclet numbers highly favours axial convection over radial diffusion. With the passage of the frontal discontinuity through the interface and into phase II, mass transfer in the porous matrix system degenerates (in this model) into a cylindrically symmetrical radial

movement in the positive r* (or r) direction. Thus, solute build-up within the porous matrix subsystem is as depicted in Figure 6 wherein the solute concentrations at various times T are plotted as a function of axial distance at r* = 1.00 (i.e., r = $2r_o$) within phase II. The diffusive nature of the evolution of concentration profiles in Figure 6 is obvious.

Figure 7 illustrates the time response of point concentrations at r* = 0.25 (middle of the conduit fracture) for three positions along the axis of revolution of the cylindrical fracture. The rapid saturation of the fracture at axial positions near the input is clearly evident, as is the gradual increase in rise times of solute buildup as points further downstream from the input are considered.

Figure 8 displays the buildup in time at a fixed axial position (Z* = 1.0) within the porous matrix subsystem for two different radial positions (r* = 1.0 and r* = 1.5). Clearly, the time response in phase II is considerably more gradual than the time response in phase I. An analysis of the concentration buildup profiles of Figure 8 indicates that a first order exponential curve may be fitted to the response function of the porous matrix subsystem (i.e., $C^{II}(t) \sim e^{kT^*}$ where k is a constant).

Figures 9 to 11 illustrate the solute buildup within the coupled fracture/porous matrix system at three axial locations, Figure 9 representing the conditions near the input (Z* = 1), Figure 10 representing the conditions further downstream from the

source ($Z^* = 2.5$), and Figure 11 representing the conditions at the selected termination point for the numerical analysis of the current model ($Z^* = \frac{L}{2r_o} = 5.0$, at which axial position $\frac{\partial C}{\partial Z}$ was set equal to zero in the boundary conditions). On each of the three figures, solute concentration is plotted against radial position for several values of time T. The advance with time of the leading edge of the frontal discontinuity of solute concentraton within the system is readily seen, as the combined effects of convection and diffusion within the conduit fracture subsystem, radial diffusion within the porous matrix subsystems, and coupling restraints between the two subsystems simultaneously enact to eventually result in total solute saturation becoming apparent within the coupled system at very large T in the following sequence.

a) High vlues of solute concentrations become apparent near the input (Figure 9) at early times. These concentrations are transported rapidly downstream within the conduit fracture due to the preferential convective transport mechanism and less rapidly radially outwards to the interface boundary.

b) For the values of Peclet numbers selected in the current model, some intrusion of solute into the porous matrix is apparent after a short passage of time near the source (Figure 9), after a longer passage of time downstream from the source (Figure 10) and

after a considerably longer passage of time at the mathematical limit of the system at $Z^* = 5.0$ (Figure 11).

c) Once the solute has intruded the porous matrix subsystem, radial diffusion proceeds at a much slower rate.

d) At an extremely large value of T the entire conduit fracture/porous matrix system becomes totally saturated (i.e., Concentration = 1.0 everywhere within the system). At this point the current model is no longer valid, since, once saturation is achieved the Peclet numbers are no longer physically meaningful (i.e., Fick's First Law is no longer applicable).

Clearly, solute transport within a coupled system will be dependent upon the physical location of the interfce boundary between the two subsystems, i.e., the solute concentration profiles will be a function of the radius r_o of the conduit fracture. This influence of r_o upon the concentration profile observable within the coupled system is schematically illustrate in Figure 12. Herein are plotted the concentration profiles observed in both subsystems at T = 40 and $Z^* = 2.5$ for four values of r_o ranging from 0.05 to 0.4. The salient features of Figure 12 are:

a) As the radius increases, larger volumes of solute enter the system, and saturation occurs in a shorter time period.

b) Small bore conduit fractures display a high degree of radial uniformity, while increasingly larger bore conduit fractures display an increasingly more parabolic radial distribution within the fracture subsystem.

c) A similar feature is observed within the porous matrix subsystem with the radial diffusion for solute intrusion from a large bore fracture displaying considerably slower rise times than the radial diffusion for solute intension from a smaller bore fracture.

SUMMARY

A mathematical model has been developed for determining the solute concentration at a point within a conduit fracture/porous matrix coupled system. The governing transport equations, which consider the effects of both convection and disperson within the conduit fracture subsystem and solely dispersion within the porous matrix subsystems, have been subjected to dimensionless analysis. The governing equations of transport, including coupling equations which provide continuity across the interface boundary of the two subsystems, have been solved utilizing alternating direction implicit method techniques.

The system has been considered to possess cylindrical symmetry and the use of cylindrical coordinates (axial and radial) enable a three-dimensional model to be expressed in essentially two dimension parameters. That such cylindrical symmetry is an eminently sensible assumption is borne out by the ubiquous occurrence of concentric rings of precipated solute in field core samples of subsurface fracture/porous matrix systems (Bobba, 1966).

Because of the dimensionless analysis techniques employed in this work, the dimensionless concentration profiles resulting from this model are functionally dependent upon a set of four dimensionless numbers which may be expressed in Peclet number form. A radial and an axial Peclet number do, in fact, deermine the salient convective and diffusive transport within the conduit fracture subsystem. A radial and axial number, both of which have been treated as Peclet numbers in this analysis, determine the salient radial and axial diffusion occurring within the porous matrix subsystem.

Concentration profiles obtained from the cylindrically symmetrical transport model illustrate an almost instantaneous appearance of solute within the conduit fracture which is rapidly convected axially through the cylinder and dispersed radially towards the interface boundary. Once solute has radially intruded the porous matrix subsystems, radial diffusion which is much slower and first order in nature is involved, with the ultimate result being a fully saturated system after an extremely long time period.

The current model has considered two very simplifying assumptions, viz. the absence of any convective flow within the porous matrix subsystem and the absence of complexities resulting from chemical adsorption within the coupled system. Current modelling works is being directed towards both the effect of convective flow within the porous matrix subsystems and the influence of chemical reactions acting throughout the system (including at the interface boundary of the two subsystems). Results of these modelling efforst should be shortly forthcoming.

REFERENCES

Ananthakrishnan, V., W.N. Gill, and Allen J. Barduhn, (1965). Laminar Dispersion in Capillaries, A.I.Ch.E. Journal, Vol. 11, pp. 1063-72.

Biard, R.B., W.E. Stewart and E.N. Lightfoot, (1960). Transport Phenomena, John Willey and Sons, Inc., New York.

Bobba, A.G., and R.P. Bukata, (1980), Parametrization of contaminant transport through an anistropic unconfirmed aquifer; Nordic Hydrology, Vol. 11, pp. 187-208.

Bobba, A.G., (1966). Dissertation on Geology, Prospecting and mining of limestone at Nandini Mines, Department of Applied Geology, Govt. College of Engineering and Technology, Raipur, M.P., India.

Day, M.J., (1977). Analysis of movement and hydrochemistry of ground water in the fractured day and till deposits of the Winnipeg area, Manitoba, M. Sc. thesis, 210 pp; Univ. of Waterloo, Ontario, 1977.

Grisak, G.E. and J.F. Pickens (1980a). An analytical solution for solute transport through fractured media with matrix diffusion. Journal of Hydrology, Vol. 52, pp 47-58.

Grisak, G.E. and J.F. Pickens (1980b). Solute transport through fractured Media 1. The effect of Matrix Diffusion. Water Resources Research, Vol. 16; No. 4, pp. 719-730, 1980.

Grisak, G.E., J.F. Pickens and Cherry, J.A., (1980). Solute transport through fractured media. 2. Column Study of Fractured Till Water Resources Research. Vol. 16, No. 4, pp. 731-739.

Jost, W., (1960). Diffusion in solids, liquid and gases. Academic Press Inc., Publishers, New York.

Peaceman, D.W. and Rachford, H.H., Jr., (1955). The numerical solution of parabolic and elliptic differntial equations. S.I.A.M. Journal, Vol. 3, pp. 28-41.

Perkins, T.K. and Johnston, O.C., (1963). A review of diffusion and dispersion in polous media, Society of Petroleum Engineers Journal, March 1980, pp. 70-84.

von Rosenberg, D.V., (1969). Methods of the numerical solution of partial differential equations. Elsevier Publishing Company, Inc., New York.

Stewart, W.E., (1965). Dimensional analysis and interphase transport, Chemical Engineering Progress symposium series, No. 58, pp. 16-27.

Sauty, J.P., (1980). An analysis of hydrodispersive transport in aquifers. Water Resources Research, Vol. 6, No. 1, pp. 145-148.

Wilson, C.R. and P.A. Witherspoon, (1970). An investigation of laminar flow infractured rocks. Geotech. Rep. 70-6. Univ. of Calif., Berkeley, U.S.A.

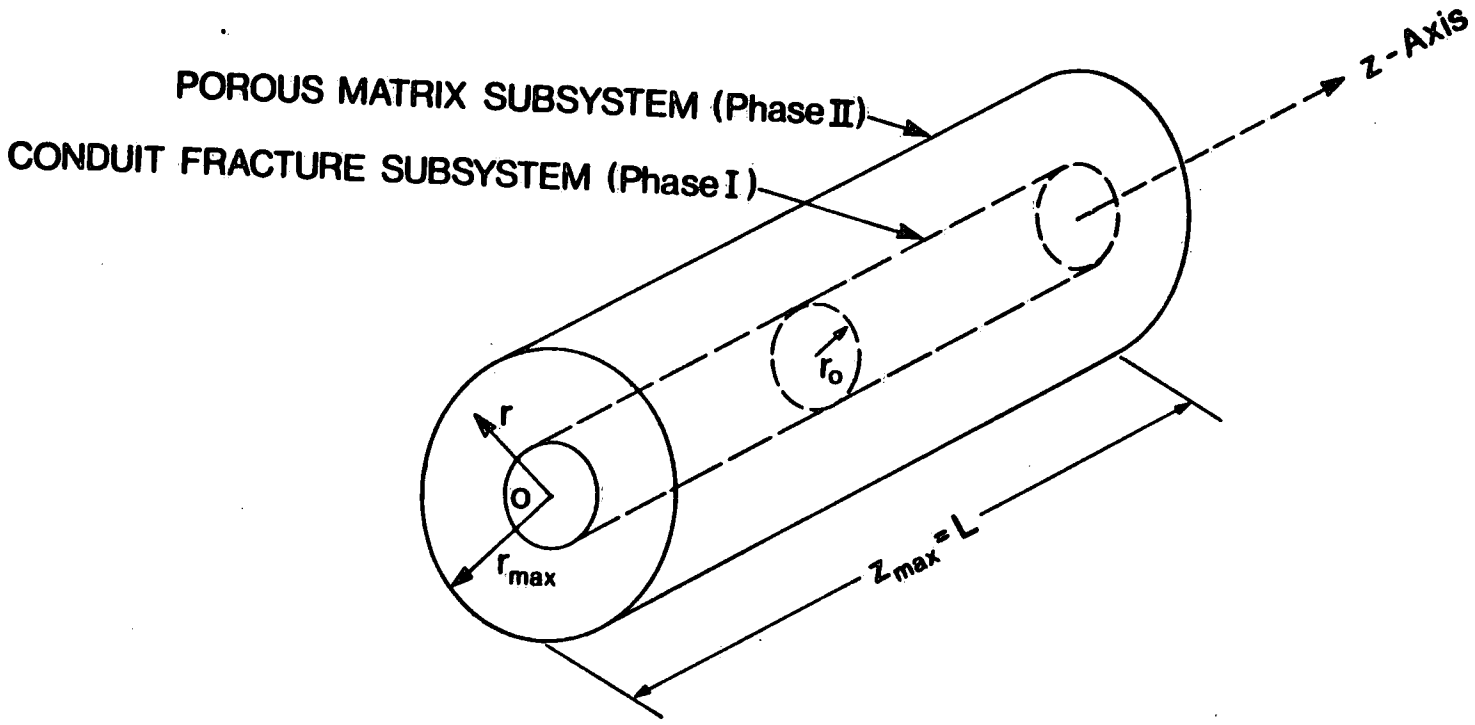

Figure 1 Cylindrically symmetrical conduit fracture/porous matrix system.

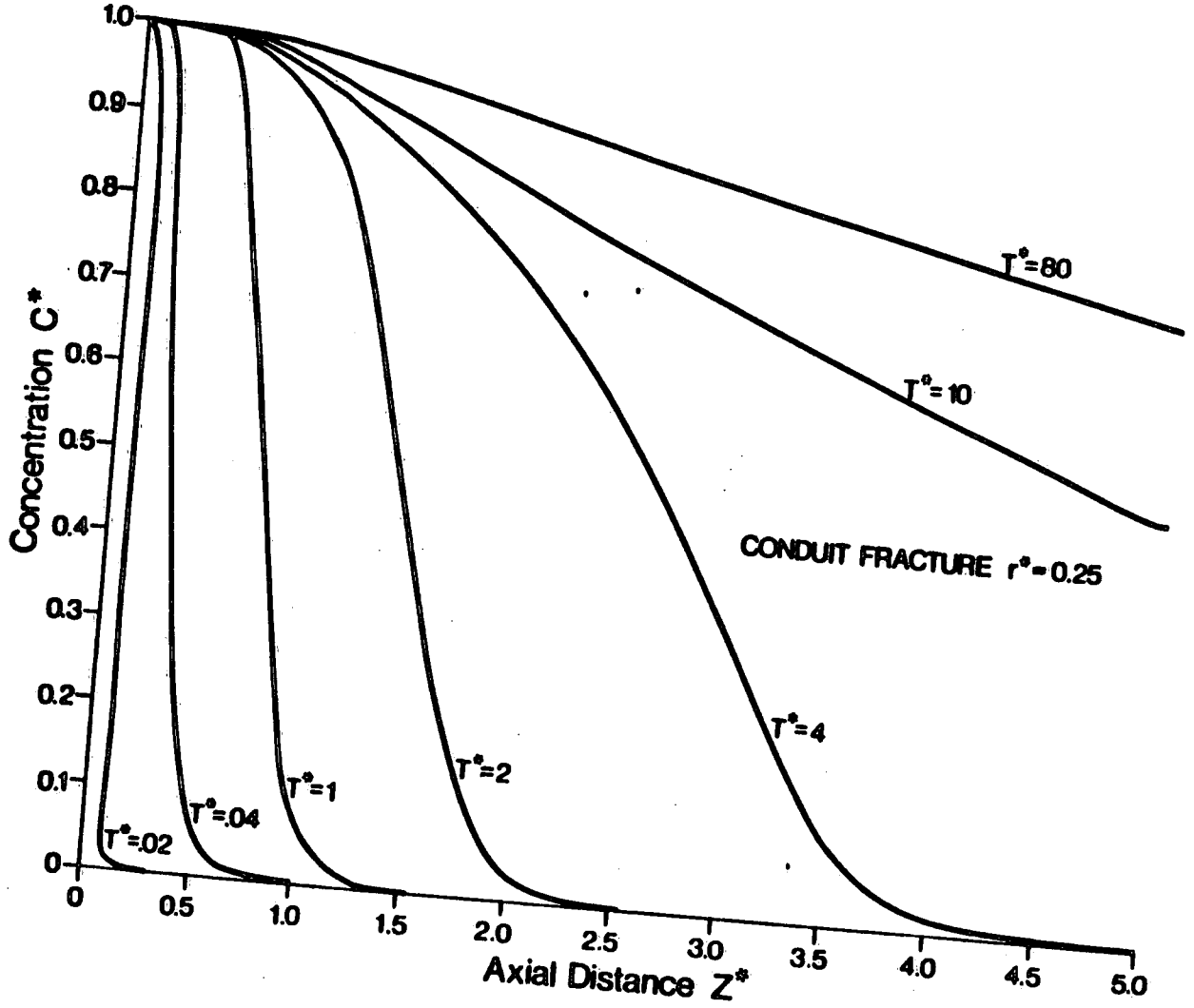

Figure 2 Transient axial solute concentration profiles in fracture at r*=0.25

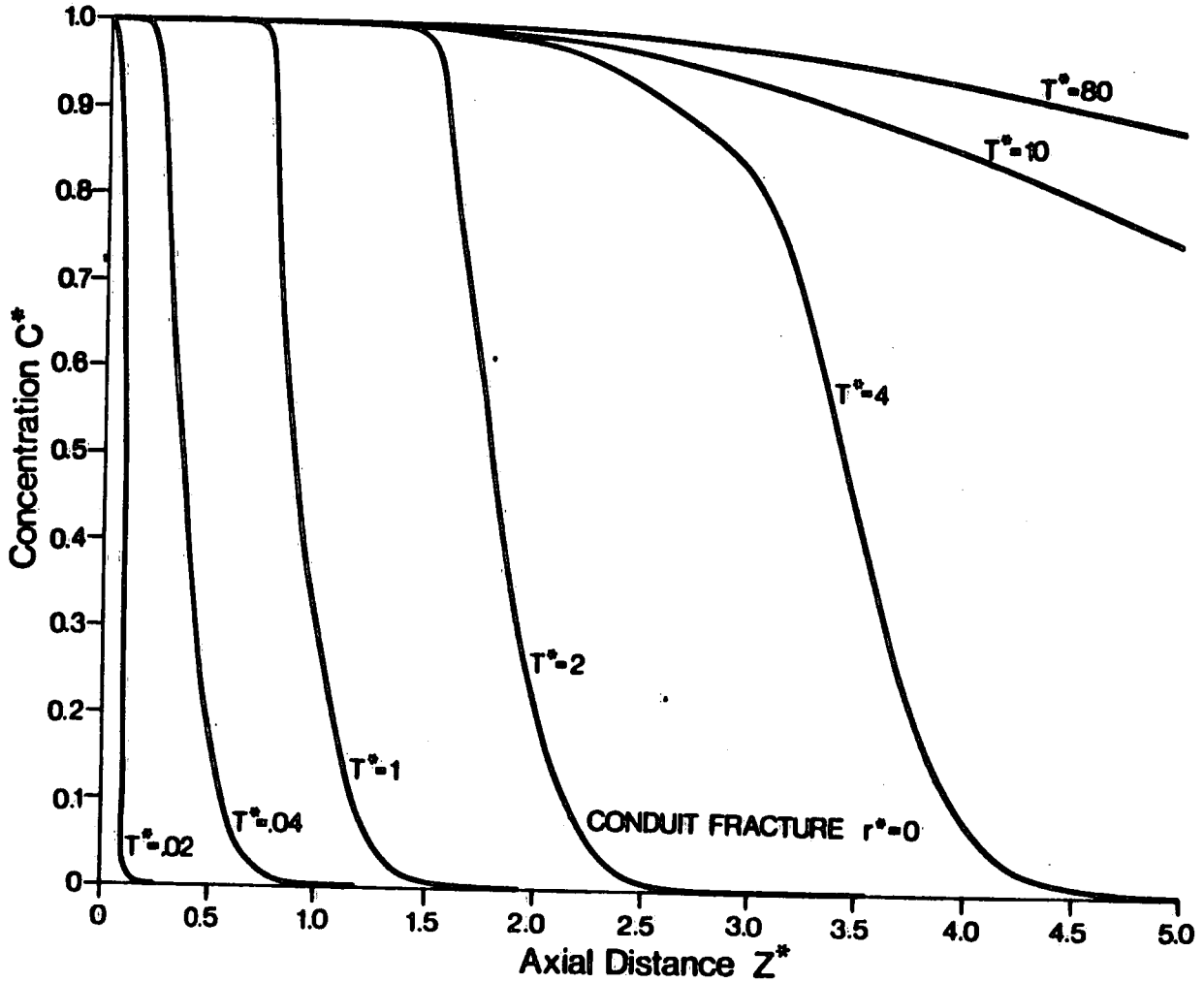

Figure 3 Transient axial solute concentrationp rofiles in midway fracture at r*=0.00.

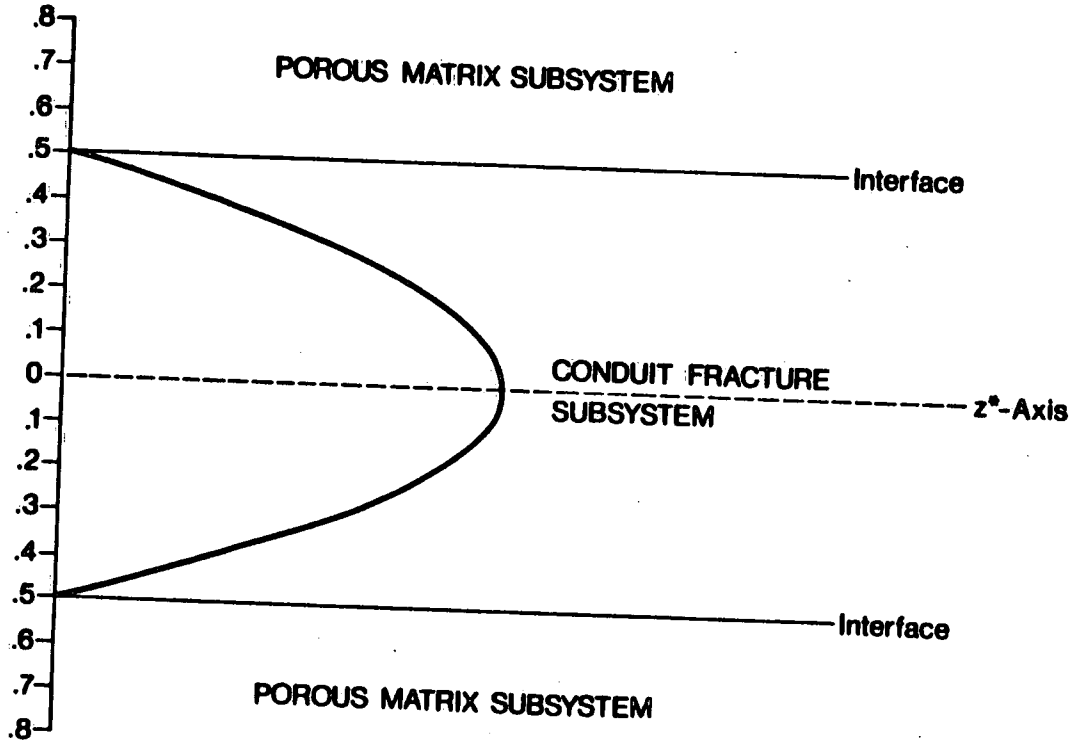

Figure 4 Parabolic velocity profile in the conduit fracture system.

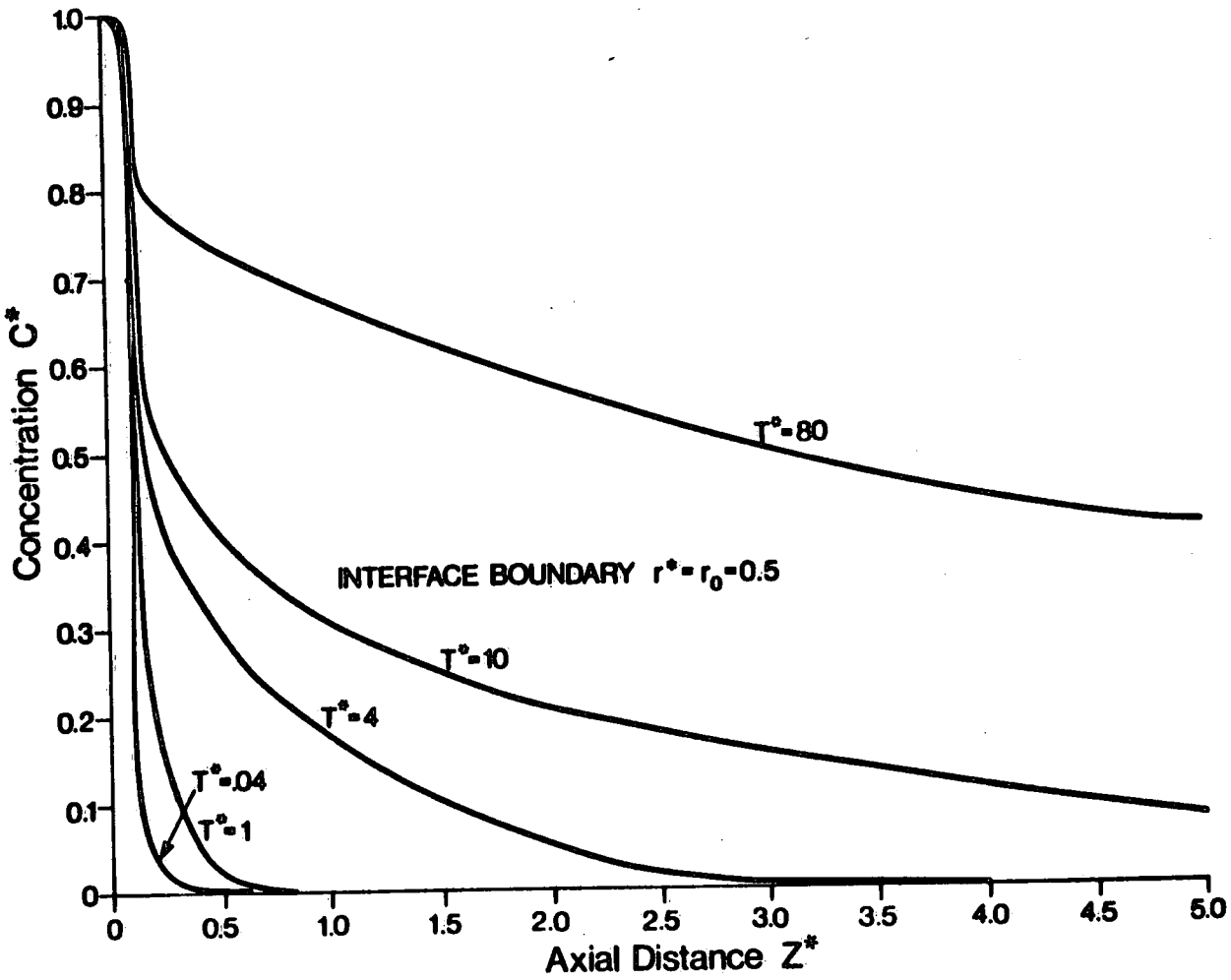

Figure 5 Transient axial concentration profiles at the interface.

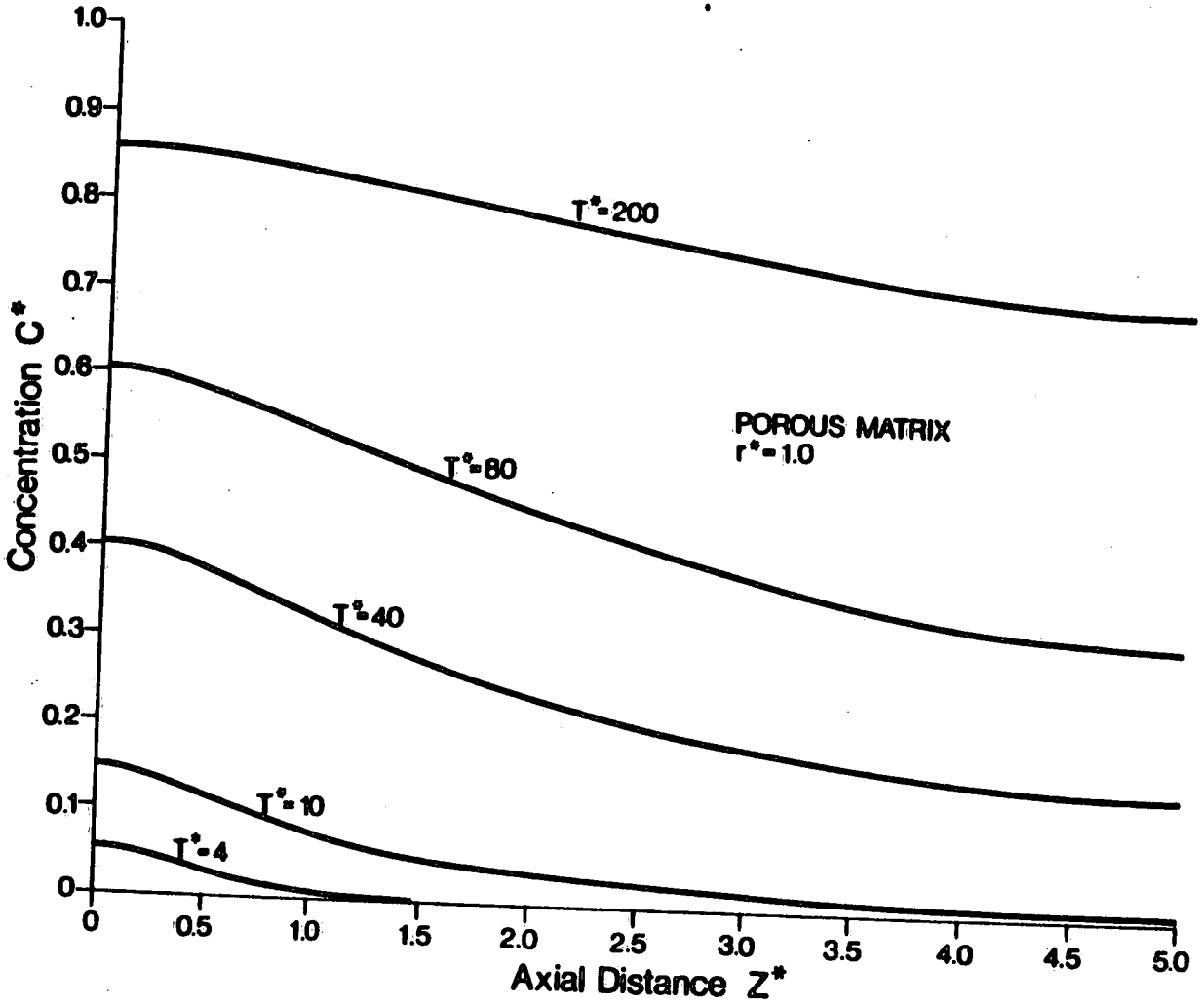

Figure 6 Transient axial concentration profiles in porous matrix at r*=1.0.

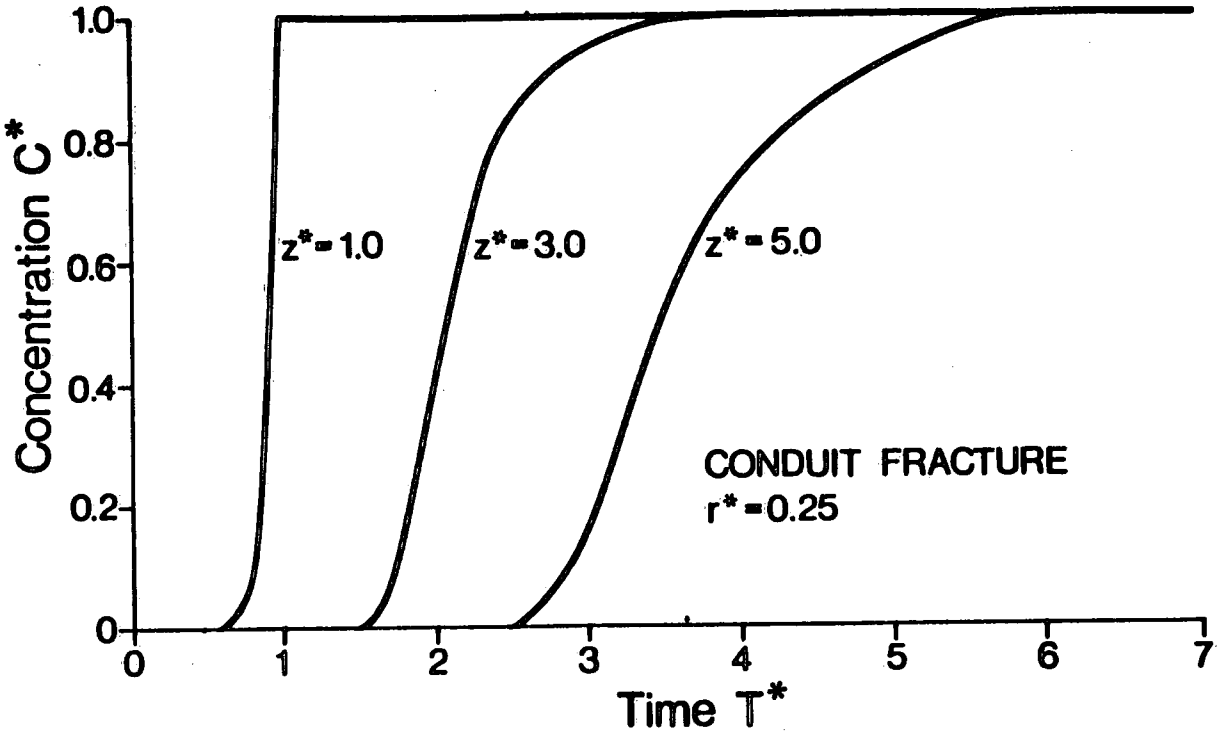

Figure 7 Time response of concentration in fracture at r*=0.25.

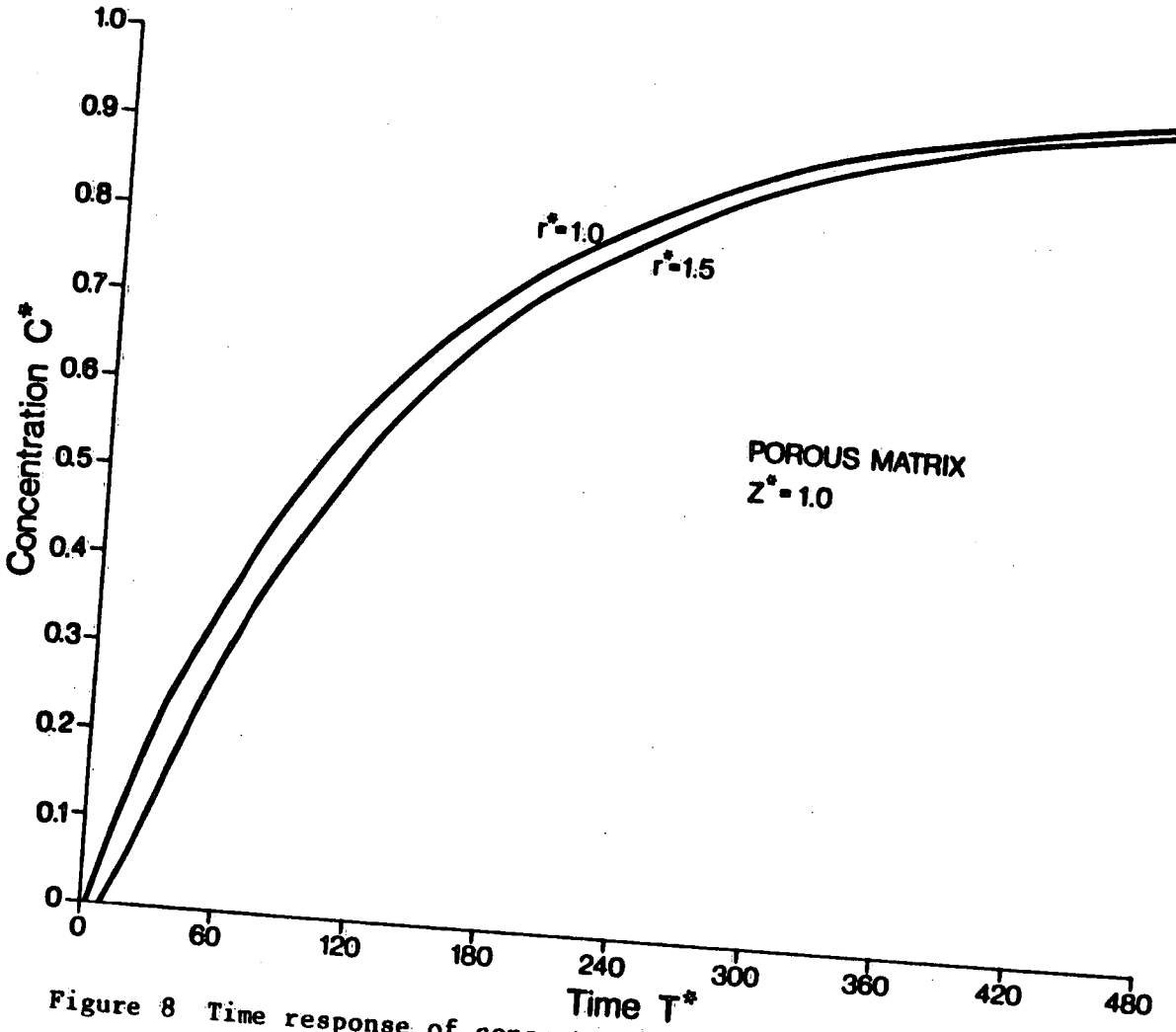

Figure 8 Time response of concentration in porous matrix at z*=1.0.

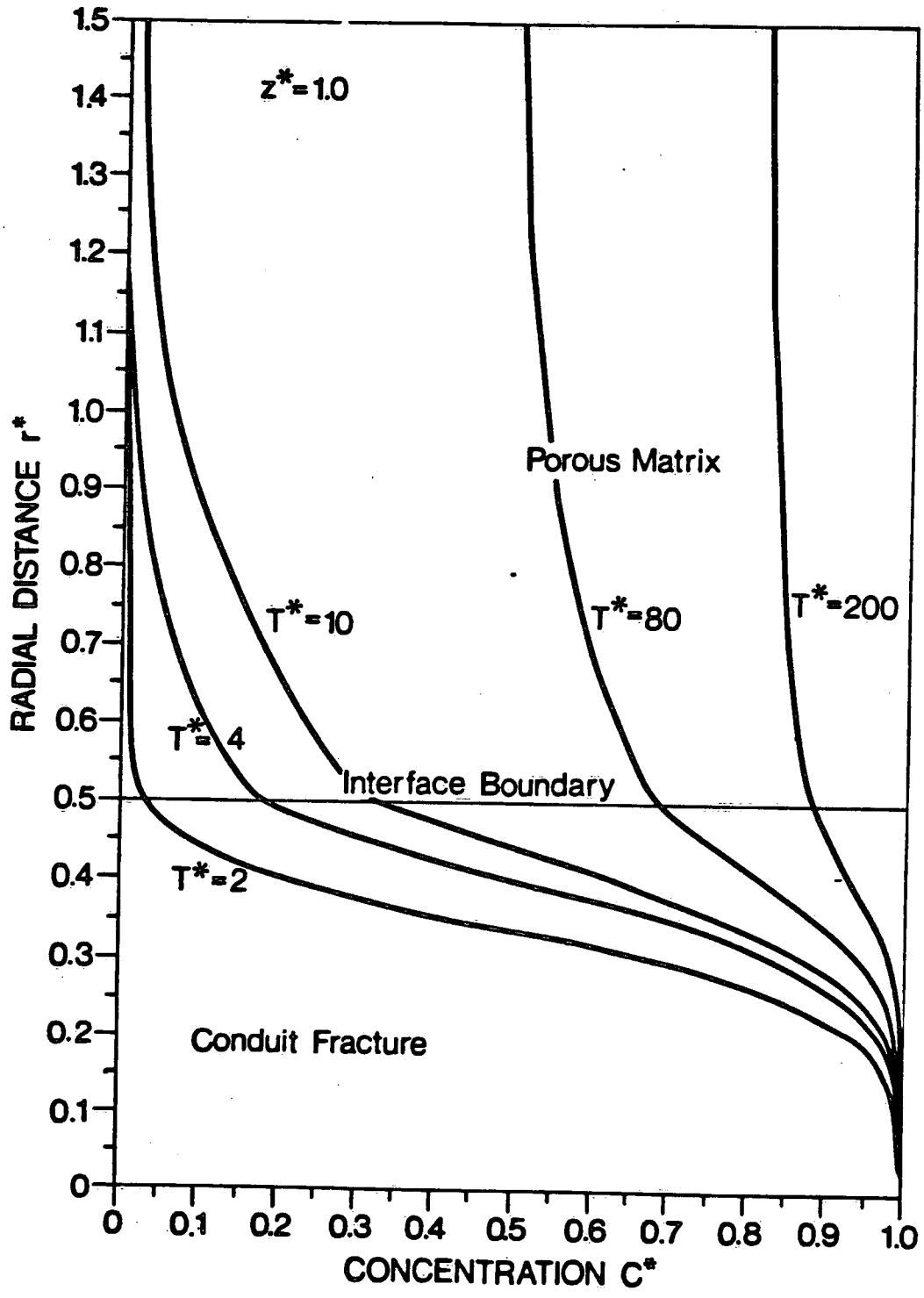

Figure 9 Transient radial concentration profiles in conduit fracture and porous matrix at z*=1.0.

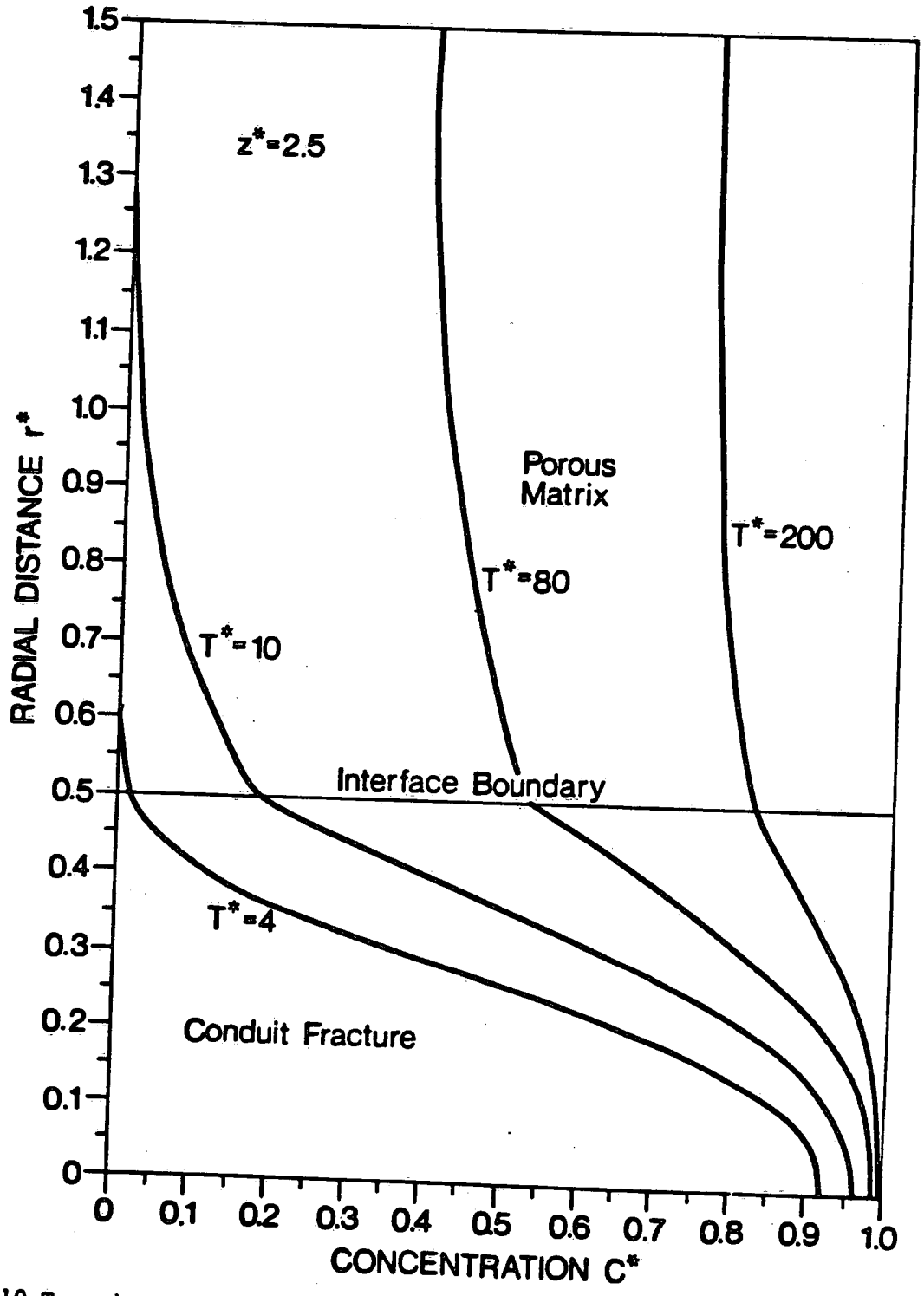

Figure 10 Transient radial concentration profiles in conduit fracture and porous matrix at z*=2.5.

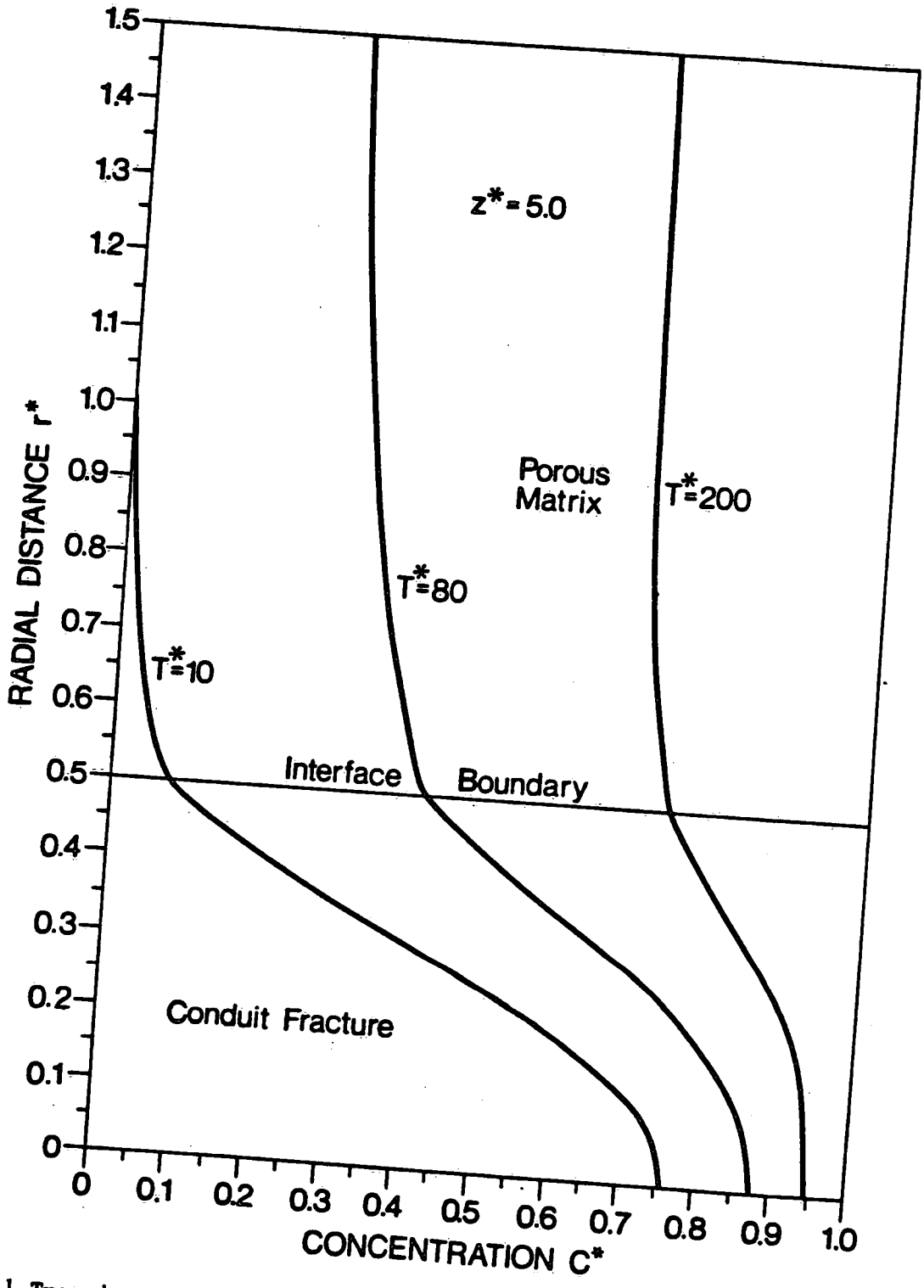

Figure 11 Transient radial concentration profiles in conduit fracture and porous matrix at z*=5.0.

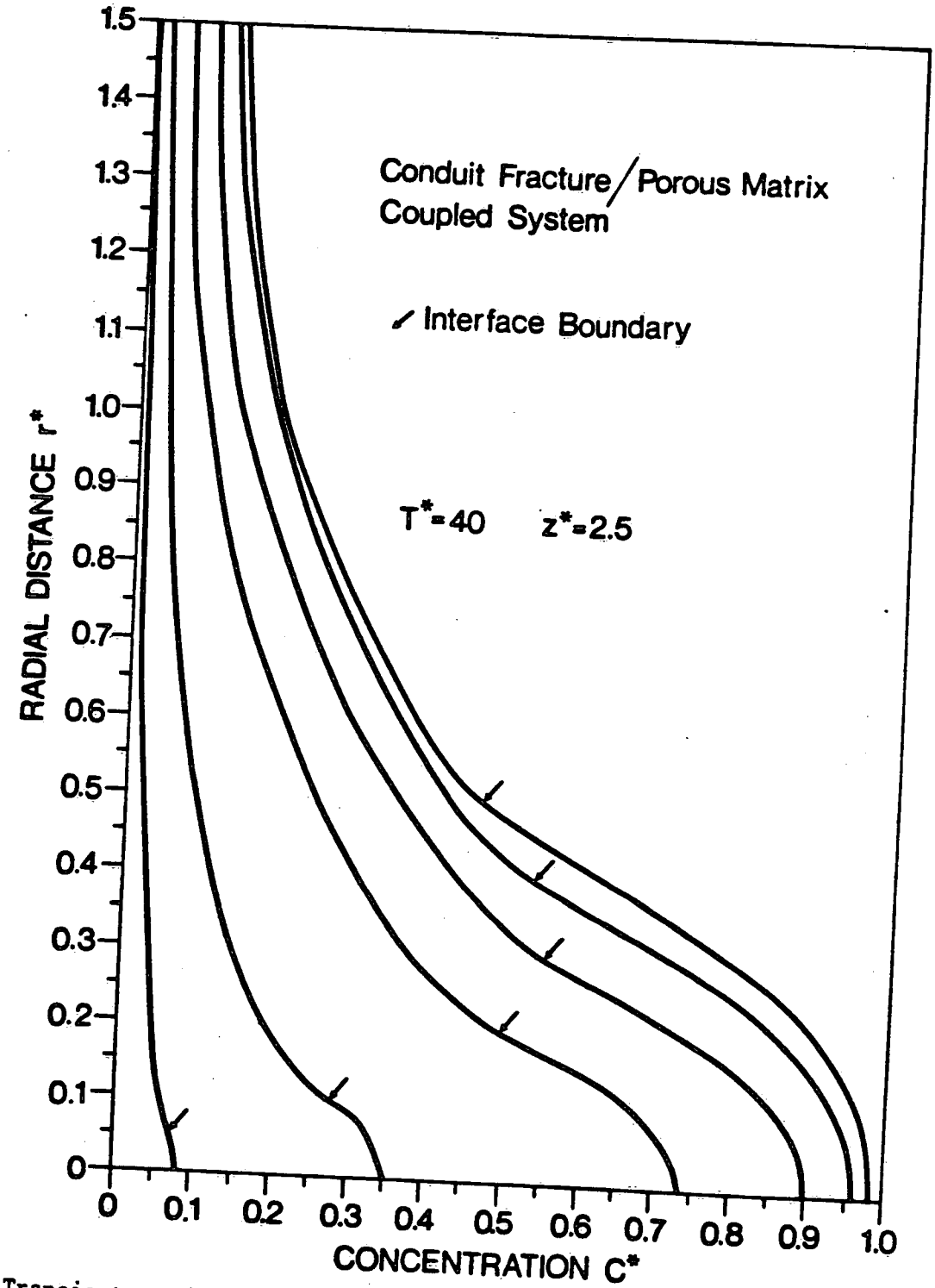

Figure 12 Transient radial concentration profiles in conduit fracture and porous matrix with different interface boundary.